

## FLOW CYTOMETRY EVALUATION OF HELA S<sub>3</sub> CELL DEATH INDUCED BY GAMMA-RADIATION

Ana Nićiforović<sup>1</sup>, Božidarka Zarić<sup>1</sup>, Aleksandra Dakić<sup>2</sup>, Nevena Tišma<sup>3</sup>, Marija B. Radojčić<sup>1</sup>

<sup>1</sup>Laboratory of Molecular Biology and Endocrinology,

VINČA Institute of Nuclear Sciences, Belgrade, Serbia and Montenegro

<sup>2</sup>Department of Genetics, University of Banja Luka, Banja Luka, Bosnia and Herzegovina

<sup>3</sup>Institute of Oncology and Radiology of Serbia, Belgrade, Serbia and Montenegro

**Summary:** In this study we followed the effects of radiation on human uterin cervix HeLa S<sub>3</sub> cells viability, morphology and DNA structure 2–96 hours after treatment with 2–10 Gy from <sup>60</sup>Co gamma radiation source. Staining of cells with Annexin V-FITC and propidium iodide showed very low degree of radiation-induced apoptosis. The prevailing form of HeLa S<sub>3</sub> cell death according to flow-cytometry, DNA fragmentation and fluorescent microscopy, was necrosis. The gamma-radiation dose necessary to induce 50% of necrosis (termed DD<sub>50</sub>) was twice higher compared to dose that induced 50% inhibition of cell proliferation (LD<sub>50</sub>). These *in vitro* data suggested, that the increase in radiation dose might eradicate tumour cells, rather than just control their proliferation and growth.

**Key words:** gamma radiation, cell death, HeLa cells, cytometry, DNA fragmentation

### Introduction

One of the aims of radiotherapy is to efficiently eradicate tumour cells with minimal deleterious effects to the surrounding normal tissues and minimal consequent damage to the whole organism. Radiation induced effects in different tissues are highly dependent on the particular cell's proliferative capacity (1). For example, rapidly dividing cells, such as intestinal crypt cells, bone marrow cells and spermatogonia, die within several hours to several days post treatment with relatively low doses of x or  $\gamma$ -radiation (0.5–2 Gy). This form of cell death is frequently associated with cell division, and is consequently termed mitotic or reproductive cell death (1). Further, not dividing or slowly dividing cells such as lymphocytes, liver, muscle or adult nerve cells die much faster, within a few hours to

a day, after irradiation with higher (up to 10 Gy) radiation doses (2, 3). Their death is not associated with cell division, and is referred to as the interphase death. It is also found that the cultured mammalian cells usually die during the interphase after exposure to a large dose of radiation (several ten Gy).

Recent developments in cytology and molecular cell biology reveal the existence of two morphologically and biochemically different forms of cell death: apoptosis and necrosis (4, 5). Apoptosis, which is also called the controlled cell death, is an active process of cellular destruction characterized by cell shrinkage, chromatin aggregation with extensive genomic fragmentation, and nuclear pycnosis (2, 6, 7). *In vivo* phagocytes normally sequester antigenically modified apoptotic cells, preventing inflammation and damage to the surrounding tissue. The other form of cell death, necrosis, is characterized by passive cell swelling, intense mitochondrial damage with rapid energy loss and generalized disruption of internal homeostasis. This swiftly leads to membrane lyses and the release of intracellular constituents, which evoke an inflammatory reaction with local cellular infiltration, vascular damage, oedema, and injury to the surrounding tissue (4). Both forms of cell death may be triggered by ionising

Address for correspondence

Marija B. Radojčić, Ph.D.  
VINČA Institute of Nuclear Sciences  
P.O.Box 522-MBE090, 11001 Belgrade, Serbia and Montenegro  
tel. +381 (11) 245-82-22 ext.304  
fax +381 (11) 344-01-00  
www.vin.bg.ac.yu  
E-mail: marija@rt270.vin.bg.ac.yu

radiation (8, 9). The relation between apoptosis and necrosis, as defined by cytologists and the reproductive and interphase death, examined by radiation biologists, is not simple. For example, irradiated intestinal crypt cells, thymocytes, lymphocytes and some carcinoma and lymphoid cell lines are susceptible to apoptosis. Apoptotic cells die in interphase, but can undergo secondary necrosis. The response to ionising radiation, depends on a number of factors such as the stage of differentiation, mutations in specific genes (such as p-53 and bcl-2) that will determine the ability of the target cells to enter apoptosis (8, 10, 11). For clinical purposes (*i.e.* irradiation of the tumour, but prevention of undesired inflammatory *sequelae*, radiation sickness and fibrosis), it is useful to investigate whether the cells of certain types are susceptible to apoptosis or necrosis, as well as to determine the time and dose dependence of the process.

In this paper we study  $^{60}\text{Co}$  gamma-radiation induced cell death of HeLa S<sub>3</sub> human uterine cervix epitheloid carcinoma cells, which is one of the most common gynaecological malignancies in the female population. The form of radiation-induced cell death is determined according to cytological, biochemical and morphology criteria, as well as its time course and the radiation dose that kills 50% of cells (DD<sub>50</sub>).

## Material and Methods

### *Chemicals and Cell lines*

Ham's F-12 medium, foetal calf serum, glutamine, antibiotics and other cell supplies were obtained from Sigma Aldrich Chemie GmbH, Germany. Cell culture bottles and other sterile dishes were purchased from Nunk, Denmark. Annexin V-FITC kit was obtained from Travigen Inc., Gaithersburg, MD, USA. Human uterine cervix epitheloid carcinoma cell line HeLa S<sub>3</sub> (CCL-2.2) was purchased from American Type Culture Collection, Rockville, MD (12). Cells were grown as monolayers in 25 cm<sup>2</sup> culture bottles supplied with 5.5 mL of Ham's F-12 medium containing 15% foetal calf serum, 2 mmol/L glutamine, penicillin (25 IU/mL) and streptomycin (25 µg/mL) at 37 °C under 5% CO<sub>2</sub> atmosphere.

### *Analysis of cell growth*

For analysis of cell growth and spontaneous cell death in culture, cells were seeded at a density of  $16 \times 10^3$  cells/cm<sup>2</sup>. Cell growth, viability and morphology were followed for 8 consecutive days, by trypan blue (TBE) assay. Cells were counted at 320× magnification using Neubauer haemocytometer and Leitz-Wetzlar Orthoplan microscope. The confluence was reached on the 8th day at  $cca 170 \times 10^3$  cells/cm<sup>2</sup>. Cell viability was determined as % of cells that excluded trypan blue stain.

### *Cell Irradiation*

Cells ( $cca 10^5$  per cm<sup>2</sup>) were irradiated with gamma-rays from a  $^{60}\text{Co}$  source under the sterile conditions in the horizontal position at 37 °C. The irradiation dose was 2-, 5- or 10 Gy and the dose rate was 0.41 Gy/min, as determined by ionising chamber and Fricke dosimetry. The effects of irradiation on cell viability, morphology and genomic DNA structure were determined 2-, 24-, 48-, 72- and 96 h after irradiation.

### *Cell preparation*

Medium from each bottle was collected, cells were harvested by trypsinization (3 mL trypsin per bottle) and pooled with the medium. Cells were washed twice in PBS and pelleted at 1500 rpm for 10 min at room temperature. Samples were used for trypan blue assay, flow cytometry, *in situ* DNA staining, or for electrophoretical analysis of purified genomic DNA.

### *Flow cytometry and In situ fluorescent microscopy*

Approximately  $10^5$  cells of each sample were mixed with 100 mL of Annexin V-FITC reagent (containing 5 µL/mL Annexin V-FITC and 5 µg/mL propidium iodide), mixed and incubated at room temperature for 15 minutes in dark and then diluted with 400 µL of binding buffer. In order to detect radiation-induced cell death multiparameter measurement of the cell sample was performed using a Becton-Dickinson FACScan flow cytometer with 488 nm, 15 mW argon-ion laser. Forward and side light scattering and stain-induced fluorescence at two different wavelengths (530 nm, green and 640 nm, red) were simultaneously measured from each cell. The forward scatter (FSC) signal is proportional to the cell size, whereas the side scatter (SSC) signal is proportional to cellular granularity. Using these two parameters it was possible to discriminate HeLa cells from cell debris for data acquisition. Staining of the cells with Annexin V-FITC (Annexin) permitted identification of cells in early apoptosis, while staining of the cells with Annexin and propidium iodide (PI) permitted quantification of cells in the late apoptosis and necrosis. Data were acquired immediately after staining by analysing about 20,000 cells/sample. The data were further processed by Becton Dickinson LYSIS II software.

For *in situ* DNA staining and fluorescent microscopy, cells were stained with 0.62 mmol/L propidium iodide and 0.33 mmol/L spermin tetrachloride and incubated for 5 minutes in dark. Stained cells in several optical fields were analysed and photographed at 400× magnification using Reichert Zetopan fluorescence microscope as already described (13).

### DNA fragmentation assay

Cells were incubated in one volume of digestion buffer for 2 h at 50 °C, followed by the addition of proteinase K and digestion was continued overnight. DNA was deproteinised using the phenol/chloroform/isomyl-alcohol reagent, for three times. The aqueous layer was transferred to a new tube and precipitated with one volume of isopropanol and 1/10 volume of ammonium acetate overnight at 4 °C. The DNA pellet was washed three times with ice-cold 95% ethanol and dried at room temperature. The final DNA pellet was resuspended in 20  $\mu$ L TE buffer and the concentration of DNA was determined spectrophotometrically. Electrophoresis of 4–10  $\mu$ g of each DNA sample, was carried out for 90 min at 50 V at 4 °C on 2% agarose gel containing 0.1  $\mu$ g/mL ethidium bromide. Gels were photographed under UV transillumination using Polaroid 667 film or GelDoc apparatus.

## Results

### Analysis of cell growth and spontaneous cell death in culture

HeLa S<sub>3</sub> cell growth and spontaneous cell death in culture were determined for the same time intervals and at the same cell densities that were subsequently used in cell irradiation experiments (cca  $10^4$ – $2 \times 10^5$  cells/cm<sup>2</sup>). Cell growth, viability and morphology were monitored for 8 consecutive days and the results are shown in *Figure 1*. Several days post plating were necessary to reach the log phase of cell growth, which occurred between 4<sup>th</sup> and 8<sup>th</sup> day of cell growth. The confluence was reached on the 8<sup>th</sup> day post plating, at the cell density of cca  $170 \times 10^3$  cells/cm<sup>2</sup>. Further incubation led to the decrease in cell number (not shown). The analysis of morphological features of HeLa S<sub>3</sub> cells by TB assay showed that approximately 5–10% of all cells were TB positive at all cellular densities. The similar result was obtained by propidium iodide (PI) staining, which is excluded from the cells with intact plasma membranes (14). The TB positive cells are either in the late stage of apoptosis or die by necrosis, according to morphological criteria.

To distinguish between those two possibilities, we analysed the fragmentation pattern of cellular DNA for days 5, 6, 7 and 8 post plating on 2% agarose gel (*Figure 2*). Fragmentation of HeLa S<sub>3</sub> cell DNA to a high molecular size ( $\geq 8$  Kb) was visible at all time points analysed, but the internucleosomal ladder was not seen. The apoptotic process in epithelial cells may not always be followed by internucleosomal fragmentation, but rather with the appearance of large DNA fragments (15). However, a slight DNA smear containing DNA fragments with molecular sizes of cca 0.1–8 Kb was evident on the days 7 and 8, and it may indicate the process of necrosis which occurred with prolonged incubation in culture (8).

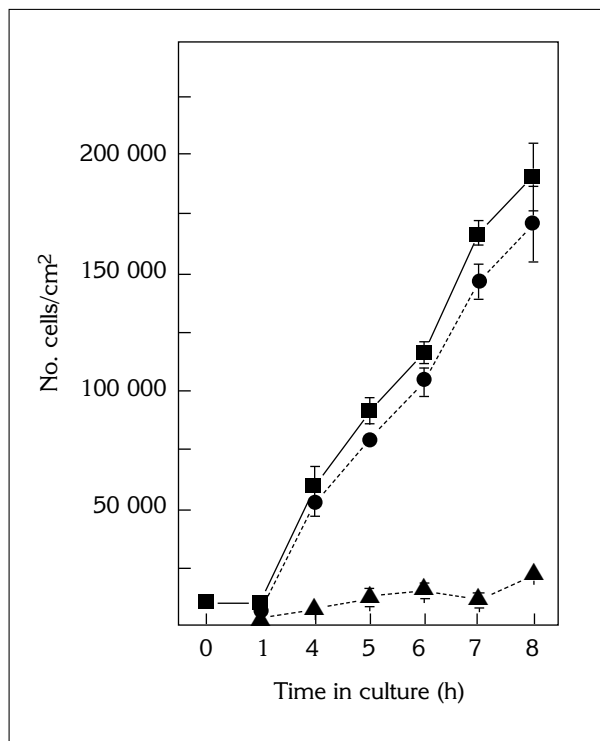


Figure 1. Growth and viability of HeLa S<sub>3</sub> cells after different time in culture. Total cells number (squares), viable cells (circles), TB positive cells (triangles). Error bars present standard error of the mean of 4 to 10 measurements for each experimental point.

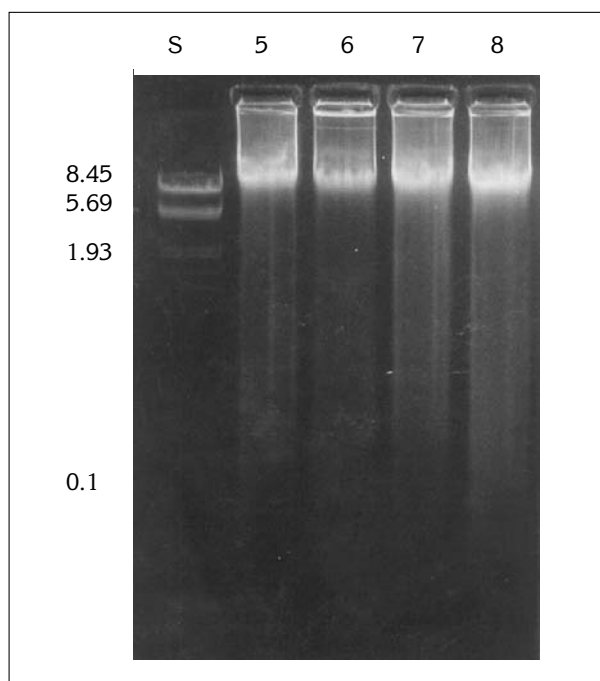


Figure 2. Agarose gel electrophoresis of DNA from HeLa S<sub>3</sub> cells cultured for different times. Lane S: DNA standard molecular size markers, lanes 5–8: DNA extracted from cells maintained in culture for 5, 6, 7 and 8 days, respectively.

*Radiation-induced cell death analysis  
by flow cytometry*

The effects of  $^{60}\text{Co}$  gamma-irradiation on HeLa S<sub>3</sub> cell viability, morphology and genomic DNA structure were followed 2-, 24-, 48-, 72- and 96 h after irradiation with 2-, 5- and 10 Gy. Multiparameter measurements of the cell samples stained with Annexin V-FITC and propidium iodide were performed using a Becton-Dickinson FACScan flow cytometer. The typical cytometric result is presented as in *Figure 3*, which shows the scatter-plots of the control and 10 Gy irradiated HeLa S<sub>3</sub> cells stained with Annexin V-FITC and PI. The number of dots in each quadrant represent cells in different states e.g. (a) viable cells, (b) cells in early apoptosis, (c) cells in late apoptosis or necrotic cells, and (d) necrotic cells and cell aggregates.

The cytometric data obtained from 20,000 cells of each  $^{60}\text{Co}$  gamma-irradiated cell sample were processed by Becton Dickinson LYSIS II software and by Origin 6.1 software. The results of evaluation of cells in different states, such as (a) viable cells, (b) cells in early apoptosis, (c) cells in late apoptosis or necrotic cells, are presented in *Table 1* (a–c) and *Figure 4* (a–f). Six to eight measurements was performed for each experimental point.

As it may be observed from *Table 1-a* and *Figure 4 a–c*, cell viability of the control samples which was

usually 90–95%, decreased with the increase in the radiation dose and with the period of culturing. Thus, 24–48 h after irradiation, the decrease of viability was cca 1–4%, and after 72h the viability dropped by cca 25%, i.e. only cca 43% of the cells were viable 72h after 10 Gy irradiation.

The  $^{60}\text{Co}$  gamma-irradiation also induced changes in integrity of HeLaS<sub>3</sub> cell membrane as well as in the cell morphology. With the increase in the radiation dose (*Table 1-b*), the percentage of cells in the state of early apoptosis increased for cca 1% during the first day post-treatment. The highest increase in the number of apoptotic cells was observed 48h after irradiation with 5 Gy, when cca. 3 % of cells were affected.

The increase in number of PI positive cells in late apoptosis or necrosis, was also observed with increase in the radiation dose (*Table 1-c*, *Figure 4 d-f*). However, during the first 2 h and 24 h post-treatment this increase was not markedly pronounced i.e. only 1–2 % of the cells were affected. After 72 h post-treatment, the number of necrotic cells was markedly increased, namely cca. 24–34 % of PI positive cells over the control, was observed at the dose of 5–10 Gy.

The *in situ* PI staining of irradiated cells showed the presence of still viable cells (*Figure 5-a*) which excluded the dye, due to intact plasma membrane. Some cells showed morphological features typical of

Table I Flow cytometry distribution of HeLa S<sub>3</sub> cells after  $^{60}\text{Co}$  gamma-irradiation calculated as means  $\pm$  S.E.M of 6–8 samples

a. Viable cells					
	% after 2 h	% after 24 h	% after 48 h	% after 72 h	% after 96 h
Control	93.09 $\pm$ 0.84	92.97 $\pm$ 0.51	92.81 $\pm$ 1.17	82.73 $\pm$ 1.75	72.26 $\pm$ 5.87
2 Gy	94.66 $\pm$ 0.93	92.35 $\pm$ 1.11	89.31 $\pm$ 2.20	71.94 $\pm$ 5.99	65.88 $\pm$ 0.58
5 Gy	95.00 $\pm$ 0.80	91.57 $\pm$ 1.90	88.09 $\pm$ 1.81	61.79 $\pm$ 5.59	49.05 $\pm$ 0.78
10 Gy	93.58 $\pm$ 0.72	93.15 $\pm$ 0.80	86.99 $\pm$ 2.45	56.94 $\pm$ 7.02	26.69 $\pm$ 7.10
b. Early apoptosis					
	% after 2 h	% after 24 h	% after 48 h	% after 72 h	% after 96 h
Control	1.67 $\pm$ 0.17	1.93 $\pm$ 0.19	1.25 $\pm$ 0.27	1.68 $\pm$ 0.42	1.56 $\pm$ 0.90
2 Gy	1.86 $\pm$ 0.33	2.08 $\pm$ 0.33	3.03 $\pm$ 0.83	1.69 $\pm$ 0.34	0.88 $\pm$ 0.15
5 Gy	1.29 $\pm$ 0.14	2.51 $\pm$ 0.63	3.17 $\pm$ 0.80	2.84 $\pm$ 1.40	1.30 $\pm$ 0.16
10 Gy	1.72 $\pm$ 0.29	2.70 $\pm$ 0.42	2.26 $\pm$ 0.69	2.50 $\pm$ 0.66	1.52 $\pm$ 0.51
c. Late apoptosis or necrosis					
	% after 2 h	% after 24 h	% after 48 h	% after 72 h	% after 96 h
Control	4.38 $\pm$ 0.75	4.82 $\pm$ 0.47	4.78 $\pm$ 0.49	15.93 $\pm$ 1.90	27.08 $\pm$ 6.05
2 Gy	3.49 $\pm$ 0.63	5.18 $\pm$ 0.92	5.92 $\pm$ 0.50	21.07 $\pm$ 3.23	33.24 $\pm$ 0.56
5 Gy	3.81 $\pm$ 0.64	5.91 $\pm$ 1.56	8.61 $\pm$ 2.00	40.01 $\pm$ 1.48	49.65 $\pm$ 0.72
10 Gy	4.84 $\pm$ 1.06	4.44 $\pm$ 0.85	10.41 $\pm$ 2.51	50.51 $\pm$ 2.21	71.79 $\pm$ 6.61

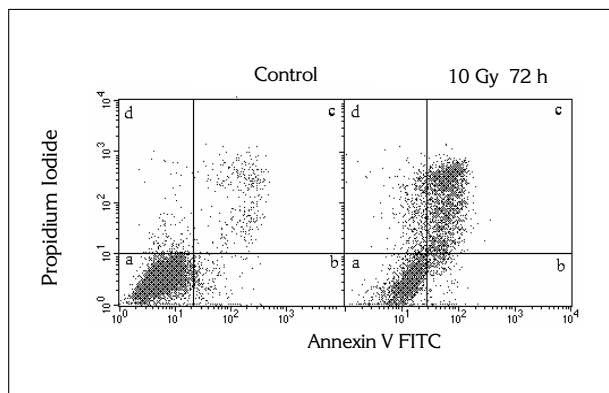


Figure 3. Flow cytometry scatter-plots of the control and <sup>60</sup>Co g-irradiated HeLa S<sub>3</sub> cells. The dots in quadrants represent: (a) viable cells, (b) cells in early apoptosis, (c) cells in late apoptosis or necrotic cells, and (d) necrotic cells and cell aggregates.

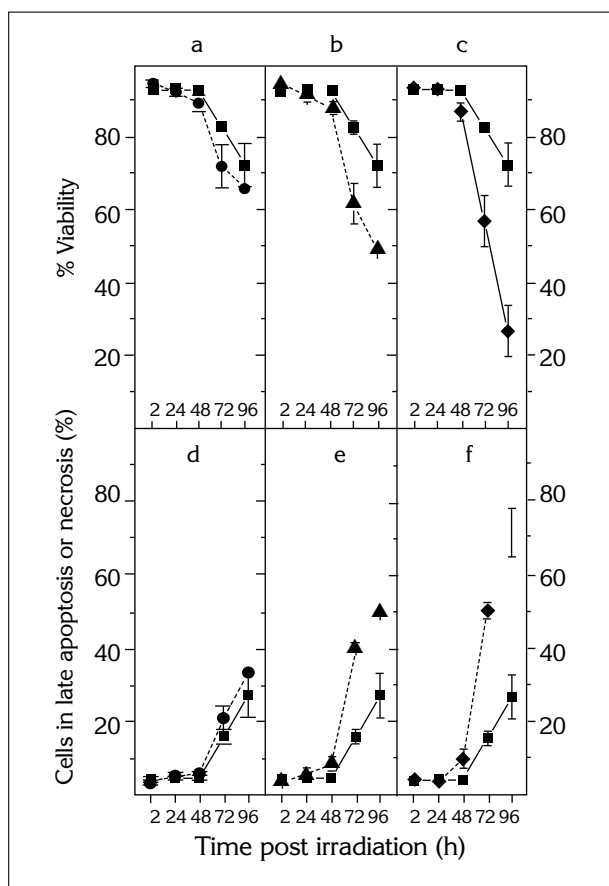


Figure 4. Time course of percent changes in HeLa S<sub>3</sub> cell viability and death after <sup>60</sup>Co g-irradiation. Viable cells (upper panel), or late apoptotic/necrotic cells (lower panel). The control samples in all panels are presented with squares and full line; samples irradiated with 2 Gy are presented with circles and dotted line (a and d); 5 Gy (triangles, and dotted lines, b and e); 10 Gy (diamonds, and dotted line, c and f). Error bars represent standard error of the mean of 6 to 8 measurements for each experimental point.

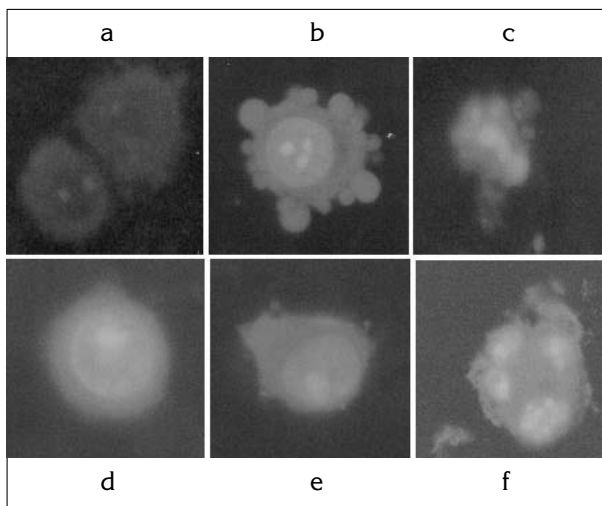


Figure 5. Fluoromicrographs of HeLa S<sub>3</sub> cells stained in situ with propidium iodide after <sup>60</sup>Co g-irradiation. Viable cells (a), apoptotic cells (b, c), necrotic cells (d, e), and cell agglomerates (f).

apoptosis, such as cell membrane blabbing and fragmentation of DNA to apoptotic bodies (Figure 5-b, and 5-c). However, some cell morphology patterns resembled cell necrosis i.e. swelled cytoplasm, ruptured membranes etc. (Figure 5-d and 5-e). In some cases cell aggregates were observed, resembling structures described as mitotic catastrophe (16).

*Electrophoretic analysis of purified genomic DNA from irradiated cells*

The genomic DNA from control and irradiated samples, including attached and floating cells, was analysed on 2% agarose gel containing 0.1 µg/mL ethidium bromide. As it may be observed in Figure 6 the initial fragmentation of HeLa S<sub>3</sub> cell DNA to a high molecular size band (≥ 8 Kb) was visible in the control samples, and its intensity gradually increased with the time in culture (2–96 h, lanes 0). The fragmentation was similar as the one observed in the HeLa S<sub>3</sub> cell growth curve study (Figure 2), and in the case of 96 h sample, further degradation was also observed. In the case of irradiated samples the fragmentation of HeLa S<sub>3</sub> cell DNA to a high molecular size band (≥ 8 Kb) was more pronounced even after 2h and smaller fragments (< 1 Kb) appeared. Their intensity increased with the dose (2–10 Gy), and was the most pronounced 72h after irradiation. However, the most interesting result was obtained 96 hours post irradiation, when, the large ≥ 8 Kb DNA fragment was further degraded to cca 1.5 Kb and cca 0.7 Kb fragments. It correlated well with the highest percent of dead cells obtained by cytometry (Table 1-c).

## Discussion

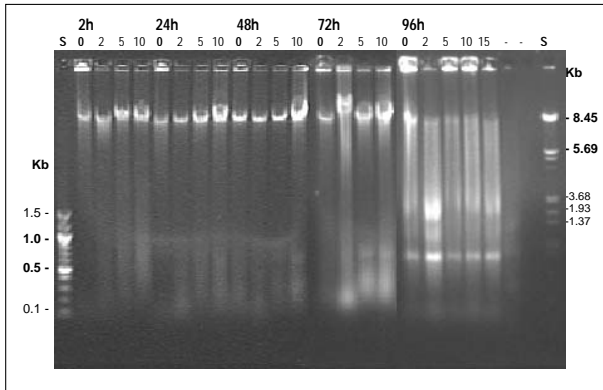


Figure 6. Agarose gel analysis of genomic DNA extracted from  $^{60}\text{Co}$  g-irradiated HeLa S3 cells. Lanes S: DNA standard molecular size markers; lanes 0–10: genomic DNA pattern of samples irradiated with 0, 2-, 5- or 10 Gy, isolated after the time indicated above (2-, 24-, 48-, 72-, or 96 hours, respectively).

Epitheloid carcinoma of uterine cervix is one of the most frequent malignancies in human population (17, 18). It is usually treated surgically in combination with subsequent radiation therapy with the aim to achieve complete eradication of the tumour (19, 20). It is well established that ionising radiation causes complex chemical and biological changes within the irradiated cell, with the final result that is highly dependent on the radiation dose applied. Thus, the irradiation with clinically relevant doses may lead to either mitotic inactivation, rendering cells incapable of further divisions (1), or may cause the actual cell death either by apoptosis or necrosis (8–10). While the cell proliferative arrest may enable tumour size control, the more preferable outcome of radiation therapy is actual cell death and complete eradication of the tumour. In addition to that, apoptosis is more favourable form of cell death, as massive necrosis may give rise to undesired post irradiation sickness and tissue fibrosis. Consequently, it is of clinical interest to know the number of tumour cells actually killed at each radiation dose and the form of cell death induced under the chosen set of conditions.

In this paper, we have quantified and classified spontaneous and  $^{60}\text{Co}$  radiation-induced death of HeLa S<sub>3</sub> cells derived from human uterine cervix epitheloid carcinoma. The growth curve of HeLa S<sub>3</sub> cells shows sigmoid-like shape, with the population doubling time about 24 h, in accordance with the data previously reported by Altman (1). The culture reaches confluence at the density of  $180 \times 10^3$  cells/cm<sup>2</sup>, which is close to the plateau density reported for the original HeLa cell clone by Freshney (21). The viability of HeLa S<sub>3</sub> cells is cca 83–93 % for the log phase of growth, and 72% for the plateau region, which is somewhat below the values reported by the ATTC pro-

ducer (12). Also, the number of propidium iodide (PI) positive HeLa S<sub>3</sub> cells increase from 5% to cca 25 % with the culturing time, indicating that certain number of cells was dying spontaneously *in vitro*. The respective profile of the genomic DNA, reveals that initial DNA fragmentation to a high molecular size ( $\geq 8$  Kb) occurs on days 5–8 post plating. According to the literature, the formation of 300 kb DNA fragments (corresponding to chromatin rosettes) and the rapid cleavage of these fragments into 50 kb solenoid fragments (corresponding to chromatin loops), may be among the earliest events in the apoptotic process (15, 22). Further degradation of these fragments into smaller oligonucleosomal fragments is not considered to be essential for the apoptotic process (15, 22). Under some other conditions, such as cell starvation, or treatment by antitumour drugs, internucleosomal ladder is also seen in HeLa cells (22). Under our experimental conditions the DNA fragment  $\geq 8$  Kb is not further degraded with time, and does not show internucleosomal ladder. Instead, a smear like pattern is observed, along with the concomitant slight decrease in cell viability. Taken together these observations show a slight cell culture deterioration with time and the DNA smear is taken as an indication of secondary necrosis (8, 22).

Bearing in mind the results of the cell growth experiment, all cell irradiation experiments are performed starting with cell density of cca  $5 \times 10^4$  cells/cm<sup>2</sup>. Cells are irradiated with 2–10 Gy from  $^{60}\text{Co}$ -source at the dose rate of 0.41 Gy/min. The dose range is chosen based on the local tumour control dose for squamous cell carcinoma, which is reported to be 60–70 Gy and which tends to be administered in 2 Gy portions (23). The irradiated HeLa S<sub>3</sub> cell cultures is followed for four consecutive days i.e. through approximately three proliferation cycles. The data obtained by the flow-cytometric analysis of 20,000 cells/sample of  $^{60}\text{Co}$ -irradiated HeLaS3 show significant decrease in cell viability both with the increase in radiation dose and with the incubation time. In overall, the process seems rather slow, and the maximum of cca 25–45% of radiation-induced cell death is observed with the doses of 5 Gy and 10 Gy after 72h and 96 h. The number of Annexin-positive/PI-negative cells, i.e. cells in early apoptosis, is rather low at all time points studied, and reaches maximum of 3% two days after irradiation with doses of 2–5 Gy. However, 35% to 45% of cells irradiated with 10 Gy are found in the flow cytometry quadrant corresponding to the late apoptosis and/or necrosis. The genomic DNA analysis of the samples indicates that the initial DNA fragmentation to band(s)  $\geq 8$  Kb which is dominant during the first two days post irradiation, is followed by a pronounced degradation through a smear like pattern of DNA fragments of the size range 0.1–1 Kb. The process is even more pronounced 96h after irradiation, when the  $\geq 8$  Kb DNA fragment is further degraded through a smear like pattern, giving rise to two other DNA bands at cca

1 Kb and 3 Kb. The fluorescent microscopy of PI stained cells indicate that the most frequent morphological feature of stained cells is swelling, membrane lyses and the release of intracellular constituents.

Taken together, the flow cytometry data, the analysis of genomic DNA, and fluorescent microscopy of PI stained HeLa S<sub>3</sub> cells, suggest that the prevailing form of <sup>60</sup>Co radiation-induced cell death is necrosis. It occurs after 72–96 h in 50% of cells irradiated with the radiation dose of cca 7 Gy. The results of genomic DNA fragmentation and of HeLa cells morphology, are in quantitative agreement with the results of Bernhard (24), with the exception of the cell death form. In our study we use Annexin staining to distinguish the early apoptotic process, from the late apoptosis and necrosis. Only about 3% of apoptotic cells are detected, indicating that under certain conditions HeLa cells may still undergo apoptosis. Such conditions are starvation (22), or low-dose and low-dose-rate irradiation (25, 26). Thus, dependent on the conditions, irradiat-

ed HeLa S<sub>3</sub> cells die by either of the two processes, like reported for 9 other cervical carcinoma cell lines by Sheridan (27). The observation may be explained with the fact that some HeLa cells express human papilloma virus E6 protein known to cause p53 degradation, which may compromise radiation induced apoptotic response (28).

It is of importance to note that gamma-radiation dose which killed 50% of irradiated cells (defined as death dose 50%, DD<sub>50</sub>) was at least twice higher compared to the dose that inhibits proliferation in 50% of cells (LD<sub>50</sub>) and which is 1.75 Gy to 3 Gy (29–31). Our *in vitro* data suggest, that the increase in radiation dose may eradicate tumour cells, rather than just control their proliferation and growth.

*Acknowledgment.* The research presented in this paper is financially supported by the Ministry of Science, Technologies and Development of Republic of Serbia, Grant No. BOI-1953.

## CITOMETRIJSKA ANALIZA SMRTI HELA S<sub>3</sub> ĆELIJA INDUKOVANE GAMA ZRAČENJEM

Ana Nićiforović<sup>1</sup>, Božidarka Zarić<sup>1</sup>, Aleksandra Dakić<sup>2</sup>, Nevena Tišma<sup>3</sup>, Marija B. Radojčić<sup>1</sup>

<sup>1</sup>Laboratorija za molekularnu biologiju i endokrinologiju,

Institut za nuklearne nauke VINČA, Beograd, Srbija i Crna Gora

<sup>2</sup>Odeljenje za genetiku, Univerzitet u Banja Luci, Banja Luka, Bosna i Hercegovina

<sup>3</sup>Institut za onkologiju i radiologiju Srbije, Beograd, Srbija i Crna Gora

*Kratak sadržaj:* Praćene su promene u vijabilnosti, morfološkim karakteristikama i DNK strukturi HeLa S<sub>3</sub> ćelija karcinoma cerviksa humanog uterusa, 2–96 časova nakon ozračivanja dozama od 2–10 Gy iz <sup>60</sup>Co izvora gama zračenja. Bojenje ćelija Aneksin V-FITC-om i propidijum jodidom pokazalo je veoma nizak nivo apoptoze indukovane zračenjem. Dominantna forma smrti HeLa S<sub>3</sub> ćelija po rezultatima citometrije, morfološkim karakteristikama i načinu fragmentacije DNK, bila je nekroza. Doza gama zračenja koja izaziva ćelijsku smrt kod 50% ćelija posmatrane populacije (označena kao DD<sub>50</sub>) bila je dva puta veća od doze zračenja koja inhibira deobu kod 50% ćelija (označena kao LD<sub>50</sub>). Ovi *in vitro* podaci pokazuju da povećanje doze zračenja može ubiti maligne ćelije, a ne samo kontrolisati njihov rast.

*Cljučne reči:* gama zračenje, ćelijska smrt, HeLa ćelije, citometrija, fragmentacija DNK

## References

1. Altman KI, Gerber GB, Okada S. eds. Radiation Biochemistry: Radiation-induced Death. New York: Academic Press, 1970: 247–307.
2. Crompton NEA. Programmed Cellular Response in Radiation Oncology. Acta Oncol 1998; 37 Suppl 11: 1–49.
3. Ross GM. Induction of cell death by radiotherapy. Endocr Relat Cancer 1999; 6: 41–44.
4. Raffray M, Coheng M. Apoptosis and Necrosis in Toxicology. A Continuum or Distinct Modes of Cell Death? Pharmacol Ther 1997; 75: 159–77.
5. Kam PCA, Ferch NI. Apoptosis: mechanisms and clinical implications. Anaesthesia 2000; 55: 1081–93.
6. Kerr JFR, Wyllie AH, Currie AR. Apoptosis. a basic biological phenomenon with wide-ranging implications in tissue kinetics. Br J Cancer 1972; 26: 239–57.
7. Wyllie H. Glucocorticoid-induced thymocyte apoptosis is associated with endogenous endonuclease activation. Science 1980; 284: 555–6.
8. Szumiel I. Ionizing radiation-induced cell death. Int J Radiat Biol 1994; 66: 329–41.

9. Dewey CW, Ling CC, Meyn RE. Radiation-induced Apoptosis. Relevance to Radiotherapy. *Int J Radiat Oncol Biol Phys* 1995; 33: 781–96.
10. Olive PL, Durand RE. Apoptosis: an indicator of radiosensitivity in vitro? *Int J Radiat Biol* 1997; 71: 695–707.
11. Kyprianou N, King DE, Bradbury D, Rhee J. Bcl-2 over-expression delays radiation-induced apoptosis without affecting the clonogenic survival of human prostate cancer cells. *Int J Cancer* 1997; 70: 341–8.
12. American Type Culture Collection. ATTC Cell Lines and Hybridomas. 1994 8<sup>th</sup> ed. Rockville, MD: 5–6.
13. Zarić B, Milosavljević BH, Radojčić M. Spontaneous and Radiation-Induced Cell Death in HeLa S3 human carcinoma. *Arch Oncol* 1999; 23: 61–7.
14. Hamel W, Dazin P, Israel MA. Adaptation of Simple Flow Cytometric Assay to Identify Different Stages During Apoptosis. *Cytometry* 1996; 25: 173–81.
15. Oberhammer F, Wilson JW, Dive C, Morris ID, Hickman JA, Wakeling AE. Apoptotic death in epithelial cells. cleavage of DNA to 300 and/or 50 kb fragments prior to or in the absence of internucleosomal fragmentation. *EMBO J* 1993;12: 3679–84.
16. Bowen ID. Techniques for demonstrating cell death. In: Bowen ID, Lockshin RA. Eds. *Cell Death in Biology and Pathology*. New York: Academic Press, 1981: 379–432.
17. Devaja O, Papadopoulos A. Molecular biology of cervical cancer. *Arch Oncol* 1998; 6: 23–6.
18. Jemal A, Thomas A, Murray T, Thun M. Cancer statistics, 2002. *CA Cancer J Clin* 2002; 52: 181–2.
19. West CML, Davidson SE, Hunter RD. Evaluation of surviving fraction at 2 Gy as a potential prognostic factor for the radiotherapy of carcinoma of the cervix. *Int J Radiat Biol* 1989; 56: 761–5.
20. Wright TC, Cox JT, Massad LS, Twigg LB, Wilkinson EJ. Consensus Guidelines for the management of women with cervical cytological abnormalities. *JAMA* 2001; 287: 2120–9.
21. Freshney RI. ed. *Culture of Animal Cells: A Manual of Basic Technique*. New York: Alan R. Liss Inc, 1987: 245–56.
22. Negri C, Bernardi R, Donzelli M, Prosperi E, Scovassi AI. Sequence of events leading to apoptosis in long term cultured HeLa cells. *Cell Death Differ* 1996; 3: 425–30.
23. Kagei K, Shirato H, Nishioka T, Kitahara T, Suzuki K, Tomita M. High-dose-rate intracavitary irradiation using linear source arrangement for stage II and III squamous carcinoma of the uterine cervix. *Radiother Oncol* 1998; 47: 207–13.
24. Bernhard EJ, Muschel RJ, Bakanauskas VJ, Mckenna WG. Reducing the radiation-induced G2 delay causes HeLa cells to undergo apoptosis instead of mitotic death. *Int J Radiat Biol* 1996; 96: 575–84.
25. Mirzaie-Joniani H, Eriksson D, Sheikholvaezin A, Johansson A, Lofroth PO, Johansson L, Stigbrand H. Apoptosis Induced by Low-dose and Low-dose-rate. *Cancer* 2002; 94 (4 Suppl): 1210–4.
26. Mirzaie-Joniani H, Eriksson D, Johansson A, Lofroth PO, Johansson L, Riklund-Ahlstrom K, Stigbrand H. Apoptosis In HeLa Hep2 Cells is Induced by Low-dose and Low-dose-rate Radiation. *Radiat Res* 2002; 158: 634–40.
27. Sheridan MT, West CM. Ability to undergo apoptosis does not correlate with the intrinsic radiosensitivity (SF2) of human cervix tumor cell lines. *Int J Radiat Oncol Biol Phys* 2001; 50: 503–9.
28. Scheffner M, Werness BA, Huibregtse JM, Levin AJ, Howly PM. The E6 oncoprotein encoded by human papillomavirus types16 and 18 promotes the degradation of p53. *Cell* 1993; 63: 1129–36.
29. Berry RJ. Effects of Small and Large First X-Ray Dose on the Two-Dose Recovery Pattern in HeLa S<sub>3</sub> Cells *in Vitro*. *Radiat Res* 1967; 32: 13–20.
30. Mitchell JB, Bedford JS, Bailey SM. Dose-Rate Effects in Mammalian Cells in Culture. III. Comparison of Cell Killing and Cell Proliferation during Continuous Irradiation for Six Different Cell Lines. *Radiat Res* 1979; 79: 537–51.
31. Tamamoto T, Ohnishi K, Takahashi A, Wang X, Yoshimura H, Ohishi H, Uchida H, Ohnishi T. Correlation between  $\gamma$ -ray-induced G<sub>2</sub> arrest and radioresistance in two human cancer cells. *Int J Radiat Oncol Biol Phys* 1999; 44: 905–9.

Received: December 10, 2003

Accepted: February 23, 2004